IOPscience iopscience.iop.org

Home Search Collections Journals About Contact us My IOPscience

Numerical studies of the two-leg Hubbard ladder

This article has been downloaded from IOPscience. Please scroll down to see the full text article.

2001 J. Phys.: Condens. Matter 13 433

(http://iopscience.iop.org/0953-8984/13/3/306)

View the table of contents for this issue, or go to the journal homepage for more

Download details:
IP Address: 171.66.16.221
The article was downloaded on 16/05/2010 at 04:42

Please note that terms and conditions apply.

INSTITUTE OF PHYSICS PUBLISHING JOURNAL OF PHYSICS: CONDENSED MATTER

J. Phys.: Condens. Matter **13** (2001) 433–448 www.iop.org/Journals/cm PII: S0953-8984(01)17622-8

Numerical studies of the two-leg Hubbard ladder

Zheng Weihong[1], J Oitmaa[1], C J Hamer[1] and R J Bursill[2]

[1] School of Physics, The University of New South Wales, Sydney, NSW 2052, Australia
[2] Department of Physics, UMIST, PO Box 88, Manchester M60 1QD, UK

E-mail: w.zheng@unsw.edu.au, j.oitmaa@unsw.edu.au, c.hamer@unsw.edu.au and bursill@dirac.phy.umist.ac.uk

Received 2 October 2000

Abstract

The Hubbard model on a two-leg ladder structure has been studied by a combination of series expansions at $T = 0$ and the density-matrix renormalization group. We report results for the ground-state energy E_0 and spin gap Δ_s at half-filling, as well as dispersion curves for one- and two-hole excitations. For small U both E_0 and Δ_s show a dramatic drop near $t/t_\perp \sim 0.5$, which becomes more gradual for larger U. This represents a crossover from a 'band insulator' phase to a strongly correlated spin liquid. The various features are collected in a 'phase diagram' for the model.

1. Introduction

The last decade has seen a great deal of interest in spin and/or correlated electron systems on a ladder structure formed from two coupled chains. This work has been motivated both by the discovery of real materials with $S = \frac{1}{2}$ ions forming a ladder structure [1], and because ladder systems exhibit a number of interesting and surprising properties (see e.g. the review of Dagotto and Rice [2]).

Particularly interesting behaviour may be expected if the system includes charge degrees of freedom. This can be achieved by doping, to create a system of strongly correlated mobile holes, as in the cuprate superconductors. Systems studied include $LaCuO_{2.5}$ doped with Sr [1] and $Ca_{14}Cu_{24}O_{41-\delta}$ doped with Sr [3], the latter showing superconductivity under pressure. The t–J and Hubbard models provide alternate representations of the physics of such systems, and both have been studied extensively. References to most of the existing work on the t–J ladder system, as well as the most recent evidence for the form of the phase diagram can be found in Müller and Rice [4].

We are here interested in the repulsive ($U > 0$) Hubbard model on a two-leg ladder. The first study of this system, to our knowledge, was by Fabrizio, Parola and Tosatti [5] who used a weak-coupling renormalization group approach to investigate the role of the interchain hopping $t_\perp$ in driving the system out of a Luttinger liquid phase. Earlier work, in this context, had considered a two-dimensional system of weakly coupled chains [6]. Further work [7, 8] using bosonization techniques has identified a number of possible phases which the two-leg

0953-8984/01/030433+16$30.00 © 2001 IOP Publishing Ltd Printed in the UK

Hubbard ladder may exhibit. In the notation of Balents and Fisher [8], these are denoted as CnSm where n, m represent the number of gapless charge and spin modes respectively. (Here $n, m = 0, 1, 2$ giving nine possible phases.)

Numerical studies of the Hubbard ladder have been carried out for both static and dynamic properties. The density-matrix renormalization group (DMRG) technique [9] has been used to calculate both spin and pairing correlations [10, 11], and to calculate the spin and charge gaps [11, 12] as functions of the parameters of the model. The one-hole spectral function has been obtained using exact diagonalizations [13] (limited to 2×8 sites) and the quantum Monte Carlo techniques [14]. This latter paper also reports results for two-hole spin and charge excitations. The spin gap at half-filling, obtained by the DMRG technique applied to a 2×32 lattice [11] showed a very sudden decrease near $t/t_\perp \simeq 0.5$, particularly for small U. However no finite-size scaling analysis was done and hence the spin gap was not obtained to high precision. This work was motivated in part by a need to confirm this, and in fact to look for possible evidence of a phase transition near this point, as well as by a desire to explore the form of dispersion curves for spin and charge excitations, which have not been obtained by DMRG methods.

The Hamiltonian of the Hubbard ladder is written as

$$H = -t \sum_{i,a,\sigma} (c^\dagger_{i,a,\sigma} c_{i+1,a,\sigma} + \text{H.c.}) - t_\perp \sum_{i,\sigma} (c^\dagger_{i,1,\sigma} c_{i,2,\sigma} + \text{H.c.}) + U \sum_{ia} n_{i,a,\uparrow} n_{i,a,\downarrow} \tag{1}$$

where i labels the rungs of the ladder, a (=1, 2) is a leg index, σ (=$\uparrow$, $\downarrow$) is the spin index and the operators have the usual meaning. There are several instructive limiting cases. When $U = 0$ the electrons are non-interacting and the system has two simple cosine bands of width $4t$ and separation $2t_\perp$. The system is metallic for all electron densities n, except for the case $n = 1$ (half-filling) and $t_\perp > 2t$ when there is a band gap and the lower (bonding) band is completely filled. The case is aptly referred to as a 'band insulator' [11]. On the other hand when the interchain hopping $t_\perp = 0$ (and $U > 0$) the ladder decouples to two Hubbard chains for which there are exact, but highly non-trivial solutions. The system is then in a Luttinger liquid phase, and also an insulator at half-filling.

When both $t_\perp$ and U are non-zero there are no exact results known. However, the form of the phase diagram can be reasonably inferred from the analytic and numerical calculations referred to above. A nice discussion is given by Noack *et al* [11]. In the limit of large U, doubly occupied sites are suppressed and the model reduces to a t–J ladder, with parameters $J = 4t^2/U$, $J_\perp = 4t_\perp^2/U$. The Hubbard ladder has electron–hole symmetry under the transformation

$$c_{i,a,\sigma} \to 1 - c_{i,a,\sigma}. \tag{2}$$

The phase diagram and properties of the model are thus symmetric about the $n = 1$ case. We see manifestations of this in the series for various excitation energies, discussed below.

In this paper we study the Hubbard ladder using both the method of series expansions [15–17] and the DMRG [9]. The series expansion method is complementary to other numerical methods and is able to provide ground-state properties, excitation spectra and $T = 0$ critical points to high accuracy. Another advantage is that one deals with a system in the thermodynamic limit and finite-size corrections are not needed. We have used this approach recently in studies of the t–J model on the square lattice [18] and on a two-leg ladder [19], and we refer the reader to those papers for details of the method and references to previous work. The emphasis of our work is on the half-filled case $n = 1$, and on one- and two-hole excitations from half-filling. The series method is not well suited to handling variable electron density.

We are not aware of any previous series work on the Hubbard ladder. Shi and Singh [20] have used a somewhat different series approach to study the Hubbard model on the square

lattice. Their method, which introduces an artificial antiferromagnetic Ising term into the Hamiltonian, is not appropriate here, as we do not expect any magnetic long-range order in the ladder system.

This paper is organized as follows. In section 2, we discuss briefly the methods used. In section 3, we study the system at half-filling. In section 4, we consider the system with one and two holes. The last section is devoted to discussion and conclusions.

2. Methods

The series expansion method is based on a linked cluster formulation of standard Rayleigh–Schrödinger perturbation theory. We use a 'rung basis' and write the Hamiltonian in the form

$$H = H_0 + xV \tag{3}$$

where

$$H_0 = -t_\perp \sum_{i,\sigma} (c^\dagger_{i,1,\sigma} c_{i,2,\sigma} + \text{H.c.}) + U \sum_{ia} n_{i,a,\uparrow} n_{i,a,\downarrow} \tag{4}$$

is taken to be the unperturbed Hamiltonian and

$$xV = -t \sum_{i,a,\sigma} (c^\dagger_{i,a,\sigma} c_{i+1,a,\sigma} + \text{H.c.}) \tag{5}$$

is the perturbation. Thus H_0 describes decoupled rungs, and can be solved exactly, while the intrachain hopping term couples the rungs and is treated perturbatively.

The Hamiltonian for a single rung has 16 possible states. These are shown in table 1. For $U < 3t_\perp$ the lowest-energy rung state is a spin singlet containing two electrons (state 0 in table 1). At $U = 3t_\perp$ there is a level crossing and the lowest-energy rung state becomes a doublet $S = \frac{1}{2}$ state with a single electron in a symmetric (bonding) state for $U > 3t_\perp$. The eigenstates of H_0 are then direct products constructed from the possible rung states. The ground state of H_0 for the half-filling system ($n = 1$) is the state that has each rung in a spin singlet. This is true even for $U > 3t_\perp$, as transferring an electron from a doubly occupied rung to another doubly occupied rung costs energy.

To compute the perturbation series we fix the values of $t_\perp$ and U and expand in powers of $x \equiv t/t_\perp$. Without loss of generality we set $t_\perp = 1$ to define the energy scale. The series are then evaluated at the desired value of t using standard Padé approximants and integrated differential approximants [21].

We have also carried out large-scale DMRG calculations [9]. Two different DMRG algorithms have been employed. Both are 'infinite-lattice' algorithms [9] with open boundary conditions. The first method uses a superblock consisting of the usual system and environment blocks with two added rungs in the middle. The system/environment blocks are augmented by one rung at a time and the superblocks always have even numbers of rungs. The second method is similar except that only one rung is kept in the middle, meaning that the superblocks have odd numbers of rungs. The second method allows more states to be retained in the blocks, whilst the even lattices dealt with in the first method are usually considered to be more desirable for finite-size scaling (FSS) studies. For the first method typical calculations involve ladders with up to 60 rungs, keeping up to 550 states per block. For the second method the superblocks studied typically reached 81 rungs and up to 1500 states were retained per block. It should be noted that the 'infinite-lattice' algorithm, despite its name, can be used to obtain accurate results for finite lattices, as we shall show in what follows.

Table 1. The sixteen rung states and their energies, where $u_1 = \frac{1}{2}\sqrt{[1 + U/\sqrt{(U^2 + 16t_\perp^2)}]}$, $u_2 = \frac{1}{2}\sqrt{[1 - U/\sqrt{(U^2 + 16t_\perp^2)}]}$, $\lambda_1 = \frac{1}{2}[U - \sqrt{(U^2 + 16t_\perp^2)}]$, $\lambda_2 = \frac{1}{2}[U + \sqrt{(U^2 + 16t_\perp^2)}]$, and 0 represents a hole, $\uparrow$ ($\downarrow$) represents an up- (down-) spin electron, $\updownarrow$ represents an electron pair.

State label	Eigenstate	Eigenvalue	Name
0	$u_1(\|\uparrow\downarrow\rangle - \|\downarrow\uparrow\rangle) - u_2(\|\updownarrow 0\rangle + \|0\updownarrow\rangle)$	λ_1	Singlet
1	$\frac{1}{\sqrt{2}}(\|0\downarrow\rangle + \|\downarrow 0\rangle)$	$-t_\perp$	Electron–hole bonding ($S^z_{\rm tot} = -\frac{1}{2}$)
2	$\frac{1}{\sqrt{2}}(\|0\uparrow\rangle + \|\uparrow 0\rangle)$	$-t_\perp$	Electron–hole bonding ($S^z_{\rm tot} = \frac{1}{2}$)
3	$\frac{1}{\sqrt{2}}(\|\updownarrow\downarrow\rangle - \|\downarrow\updownarrow\rangle)$	$U - t_\perp$	Three-electron antibonding ($S^z_{\rm tot} = -\frac{1}{2}$)
4	$\frac{1}{\sqrt{2}}(\|\updownarrow\uparrow\rangle - \|\uparrow\updownarrow\rangle)$	$U - t_\perp$	Three-electron antibonding ($S^z_{\rm tot} = \frac{1}{2}$)
5	$\|\downarrow\downarrow\rangle$	0	Triplet ($S^z_{\rm tot} = -1$)
6	$\frac{1}{\sqrt{2}}(\|\uparrow\downarrow\rangle + \|\downarrow\uparrow\rangle)$	0	Triplet ($S^z_{\rm tot} = 0$)
7	$\|\uparrow\uparrow\rangle$	0	Triplet ($S^z_{\rm tot} = 1$)
8	$\|00\rangle$	0	Hole-pair singlet
9	$\frac{1}{\sqrt{2}}(\|\updownarrow 0\rangle - \|0\updownarrow\rangle)$	U	An electron pair and a hole singlet
10	$\|\updownarrow\updownarrow\rangle$	$2U$	An electron pair
11	$\frac{1}{\sqrt{2}}(\|0\downarrow\rangle - \|\downarrow 0\rangle)$	$t_\perp$	Electron–hole antibonding ($S^z_{\rm tot} = -\frac{1}{2}$)
12	$\frac{1}{\sqrt{2}}(\|0\uparrow\rangle - \|\uparrow 0\rangle)$	$t_\perp$	Electron–hole antibonding ($S^z_{\rm tot} = \frac{1}{2}$)
13	$\frac{1}{\sqrt{2}}(\|\updownarrow\downarrow\rangle + \|\downarrow\updownarrow\rangle)$	$U + t_\perp$	Three-electron bonding ($S^z_{\rm tot} = -\frac{1}{2}$)
14	$\frac{1}{\sqrt{2}}(\|\updownarrow\uparrow\rangle + \|\uparrow\updownarrow\rangle)$	$U + t_\perp$	Three-electron bonding ($S^z_{\rm tot} = \frac{1}{2}$)
15	$u_2(\|\uparrow\downarrow\rangle - \|\downarrow\uparrow\rangle) + u_1(\|\updownarrow 0\rangle + \|0\updownarrow\rangle)$	λ_2	Mixed singlet

3. The half-filled case

3.1. Ground-state energy

We first consider the ground-state energy E_0 at half-filling. The series method yields an expansion of

$$E_0 = \sum_n a_n (U/t_\perp)(t/t_\perp)^n. \tag{6}$$

The series have been computed to order x^{14} for various $U/t_\perp$. The coefficients for $U/t_\perp = 8$ are given in table 2, and the other coefficients can be provided on request. The cluster data for this one-dimensional problem are trivial. The limiting factor is the size of the matrices used in obtaining the cluster energies. DMRG calculations give the ground-state energy directly for a given lattice, and finite-size scaling must be used to extract the bulk result.

In figure 1 we show our results for the ground-state energy in the half-filled case versus t for various $U/t_\perp$ obtained both by series expansions and DMRG calculations. For given t the energy increases with U as expected. For fixed U the energy decreases slowly with increasing t. The series are well converged for $t/t_\perp \lesssim 0.6$, but the convergence deteriorates rapidly at that value. The DMRG calculation is, however, well converged even for larger t and agrees well with the series results for smaller t. A remarkable feature of the ground-state energy is the sharp downturn which occurs near $t/t_\perp \sim 0.5$–0.6 for $U/t_\perp \lesssim 1$, but which becomes smoother for larger U. For the case of free electrons ($U = 0$) the ground-state energy is exactly

$$\frac{E_0}{Nt_\perp} = \begin{cases} -1 & t/t_\perp < 1/2 \\ -1 - \dfrac{2}{\pi}\left[\sqrt{(2t/t_\perp)^2 - 1} - \cos^{-1}\left(\dfrac{t_\perp}{2t}\right)\right] & t/t_\perp > 1/2 \end{cases} \tag{7}$$

Table 2. Non-zero coefficients of $(t/t_\perp)^n$ for the ground-state energy per site E_0/N, the spin gap Δ_s, the one-hole energy $\Delta_{1h}(\pi)$ and the two-hole energy $\Delta_{2h}(\pi)$ at $U/t_\perp = 8$.

n	$E_0/NJ_\perp$	$\Delta_s/J_\perp$	$\Delta_{2h}/J_\perp$
0	$-2.360679774998 \times 10^{-1}$	$4.721359549996 \times 10^{-1}$	$4.721359549996 \times 10^{-1}$
2	$-8.944271909999 \times 10^{-2}$	$-7.478019326001 \times 10^{-1}$	$3.577708764000 \times 10^{-1}$
4	$-7.055810863547 \times 10^{-2}$	$2.984040157758 \times 10^{-1}$	$2.117784192484 \times 10^{-1}$
6	$-5.448947627757 \times 10^{-2}$	$2.126553951831 \times 10^{-1}$	-1.022223221785
8	$-3.092587547718 \times 10^{-2}$	$1.030100155673 \times 10^{-1}$	$-1.054110318250 \times 10^{1}$
10	$5.006769301333 \times 10^{-3}$	$-2.047688788511 \times 10^{-2}$	$-8.623391111290 \times 10^{1}$
12	$4.598641784004 \times 10^{-2}$	$-2.168399847938 \times 10^{-1}$	$-6.784316243528 \times 10^{2}$
14	$7.235038860679 \times 10^{-2}$		

n	$\Delta_{1h}/J_\perp$
0	$-5.278640450004 \times 10^{-1}$
1	-1.447213595500
2	$-5.681892697507 \times 10^{-2}$
3	$4.190688837075 \times 10^{-1}$
4	$-2.186544916675 \times 10^{-2}$
5	$7.778879476658 \times 10^{-1}$
6	-1.450073605871
7	4.979933826800
8	$-1.393584028913 \times 10^{1}$
9	$4.115238962605 \times 10^{1}$

and, as mentioned above, the crossover represents a transition from band insulator to a conductor with gapless charge and spin excitations. We can compare our results for the ground-state energy with those of Kim *et al* [22], obtained via a variational method. These are shown in figure 1. The results are in good agreement for small $t/t_\perp$, but it appears that the variational method significantly overestimates the ground-state energy for large $t/t_\perp$.

3.2. Spin excitations

We now turn to the excitations, which we have computed directly using Gelfand's method [17]. The lowest-energy spin-excitation branch results from exciting a rung from a spin singlet (state 0 in table 1) to a triplet (any of states 5, 6, 7 in table 1). Non-zero t allows this to propagate coherently along the chain, giving rise to a triplet magnon excitation. Figure 2 shows dispersion curves $\Delta_s(k)$ for this excitation for fixed $t/t_\perp = 0.5$ and various $U/t_\perp$. For larger $t/t_\perp$ the series becomes too erratic. For all cases the energy minimum occurs at $k = \pi$. As U increases the bandwidth of the spin excitation decreases.

The excitation energy at $k = \pi$ defines the spin gap $\Delta_s \equiv \Delta_s(\pi)$. The raw data are shown in figure 3, where we plot $\Delta_s/t_\perp$ versus $t/t_\perp$ for various $U/t_\perp$. For small t our series give rather precise estimates. In the limit $t = 0$ the spin gap is $\frac{1}{2}[\sqrt{(U^2 + 16t_\perp^2)} - U]$ which is $2t_\perp$ for $U = 0$ and decreases for increasing U. Near $t/t_\perp \sim 0.4$–0.5 there is a crossover and beyond this point the spin gap for large U exceeds that for small U. For $U/t_\perp \lesssim 2$ this crossover becomes very sharp. The series extrapolations would indicate that the spin gap actually vanishes at $t/t_\perp \simeq 0.5-0.6$, but we believe that this is an artefact of poor convergence in this region. It is expected [8, 11] that at half-filling the system will have a finite spin gap throughout the phase diagram for any $U > 0$, due to 'Umklapp' processes. It is clear however that the spin gap becomes quite small for $t/t_\perp \gtrsim 0.5$.

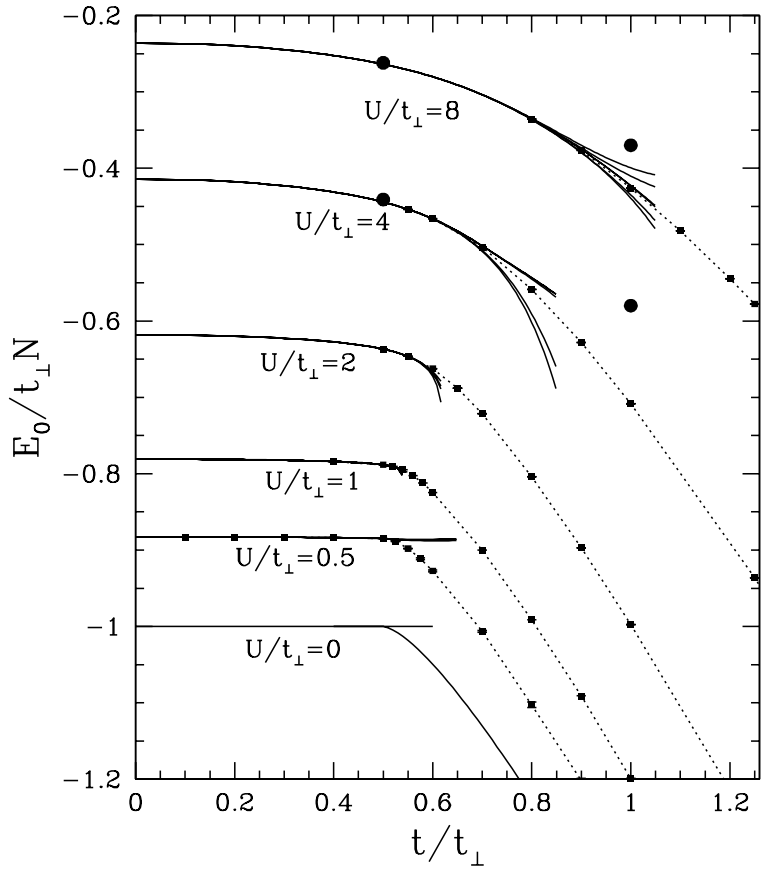

Figure 1. The ground-state energy per site as a function of $t/t_\perp$ for $U/t_\perp = 0, 0.5, 1, 2, 4, 8$. The solid lines are extrapolations of the series using different integrated differential approximants, while the points connected by dashed lines are the results of DMRG calculations. Also shown are the exact results for $U = 0$, and the results of a variational approach [22] for $U/t_\perp = 4, 8$ and $t/t_\perp = 0.5, 1$ (full circle points).

We have also used our DMRG algorithms to calculate Δ_s. In order to obtain insight into the potential limitations of DMRG methods for this problem, we consider the finite-size scaling of Δ_s in the exactly solvable $U = 0$ case. As mentioned, for $U = 0$, the system is gapped for $t_\perp > 2t$ and gapless for $t_\perp < 2t$. In figure 4 we plot Δ_s as a function of $1/N_{\rm rung}$ for three values of the ratio $t/t_\perp$. For $t/t_\perp = 0.49$ (just below the critical ratio), the system has a small spin gap, and Δ_s scales smoothly to its bulk value, the finite-size corrections vanishing as $1/N_{\rm rung}^2$ (as is to be expected for a gapped system with open boundary conditions). For $t/t_\perp = 0.51$ (just above the critical ratio), the gap suddenly begins to display a 'sawtooth' dependence on $N_{\rm rung}$, with the points of the saw scaling towards zero as $N_{\rm rung} \to \infty$. This behaviour becomes more pronounced as we move further beyond the critical ratio. It appears that multiple crossovers are occurring, with new states crossing over to the bottom of the spectrum as $N_{\rm rung}$ increases. These sawtooth oscillations are presumably due to the two-band structure: every so often it is energetically favourable for an extra electron to be added to the top band rather than the bottom band, and a crossover occurs. This oscillatory behaviour has not been exhibited before, as far as we are aware.

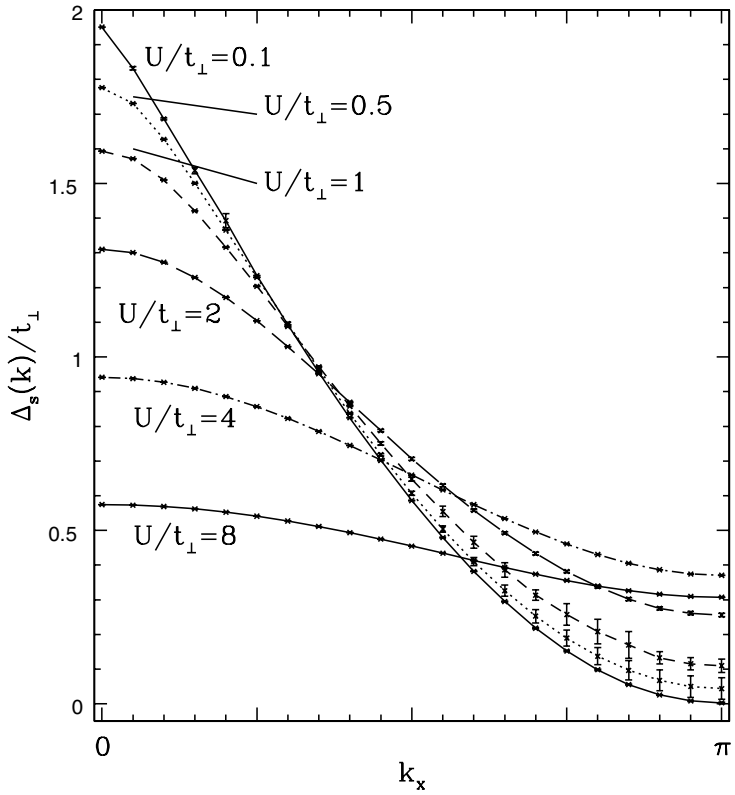

Figure 2. Spin-excitation spectra for $t/t_\perp = 0.5$ and various $U/t_\perp$, obtained from series expansions.

In order to calculate the bulk spin gap successfully with the DMRG, we must first accurately calculate Δ_s for a number of lattice sizes $N_{\rm rung}$, and then extrapolate to the bulk limit, assuming some scaling *ansatz* for the finite-$N_{\rm rung}$ corrections. An example of this is shown in table 3, where we compare DMRG and exact results for Δ_s for finite lattices and the bulk limit. In

Table 3. Comparison between exact and DMRG results for the spin gap $\Delta_s/t_\perp$ for various lattice sizes $N_{\rm rung}$ for the case of $U = 0, t/t_\perp = 0.49$. The DMRG results are obtained using the odd-rung algorithm, retaining around $m = 700$ states per block, and including the ground and first excited states in the density matrix with equal weights. The $N_{\rm rung} = \infty$ DMRG result is obtained by extrapolating the finite-$N_{\rm rung}$ DMRG results over the range $63 \leqslant N_{\rm rung} \leqslant 81$, assuming that the corrections to the bulk result scale as $1/N_{\rm rung}^2$.

$N_{\rm rung}$	DMRG	Exact
3	0.614071	0.614071
9	0.136013	0.135929
19	0.064140	0.064131
37	0.046701	0.046694
55	0.043092	0.043083
67	0.042103	0.042091
81	0.041456	0.041438
∞	0.040055	0.040000

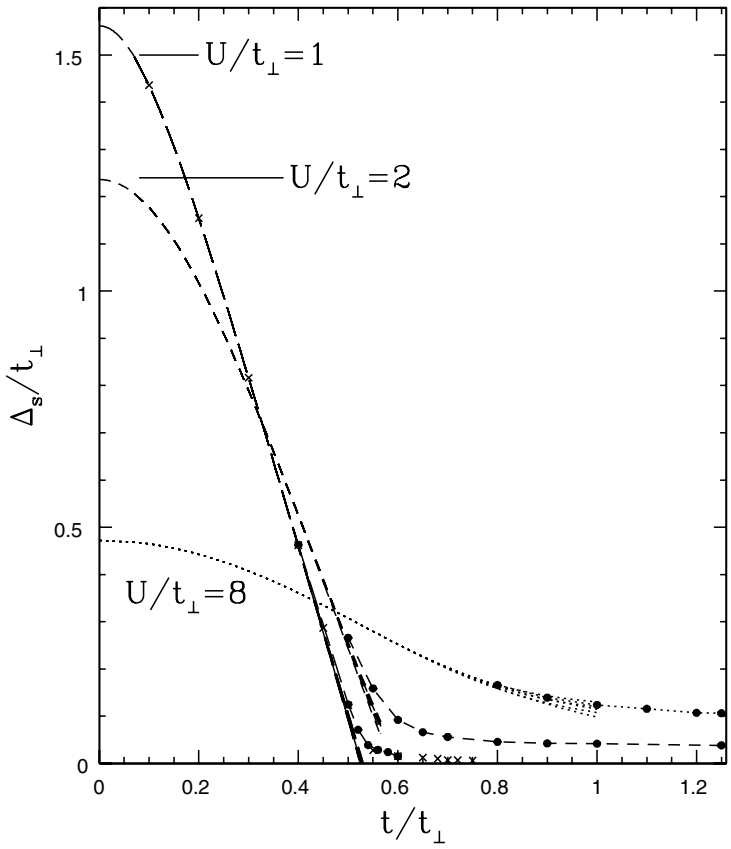

Figure 3. The spin gap Δ_s versus $t/t_\perp$ for various $U/t_\perp$. The dashed lines are extrapolations of the series using different integrated differential approximants, while the points connected by solid lines are the results of DMRG calculations. The filled circles (crosses) denote results obtained from the even-rung (odd-rung) algorithm.

this case, where the FSS is smooth, it is possible to obtain a reasonable estimate for the bulk spin gap, the real error being around 0.1%. Two potential problems emerge from our studies of gapless systems in the $U = 0$ case for $t/t_\perp > 0.5$. Firstly, because of the oscillating FSS it might be difficult to obtain accurate DMRG results for very large lattices in a regime where the gap is small or vanishing. Convergence of finite-lattice results with the number of states, m, retained per block, must be monitored over a large range of m-values. For a given lattice size, improved DMRG estimates can be obtained by using a finite-lattice algorithm [9]. However, even if highly accurate results are available for a number of lattice sizes, a second and more pressing problem is that, as a result of the oscillations or erratic FSS, extremely large lattices may be needed in order to reach a regime where a suitable scaling *ansatz* can be reliably used to extrapolate to the bulk limit, as can be seen for the gapless cases in figure 4.

Fortunately, the presence of electron repulsion smooths out the FSS, allowing reliable DMRG estimates of Δ_s some way beyond $t/t_\perp = 0.5$. In figure 5, we show the FSS of DMRG estimates of Δ_s in the $U/t_\perp = 1$ case for various $t/t_\perp$. We find that up to around $t/t_\perp = 0.55$, the corrections to the bulk results for Δ_s scale as $1/N_{\mathrm{rung}}^2$, as in the gapped case for $U = 0$. As $t/t_\perp$ is increased, however, we observe initially oscillatory or erratic FSS, followed by a crossover to linear dependence of Δ_s on $1/N_{\mathrm{rung}}$, as might be expected

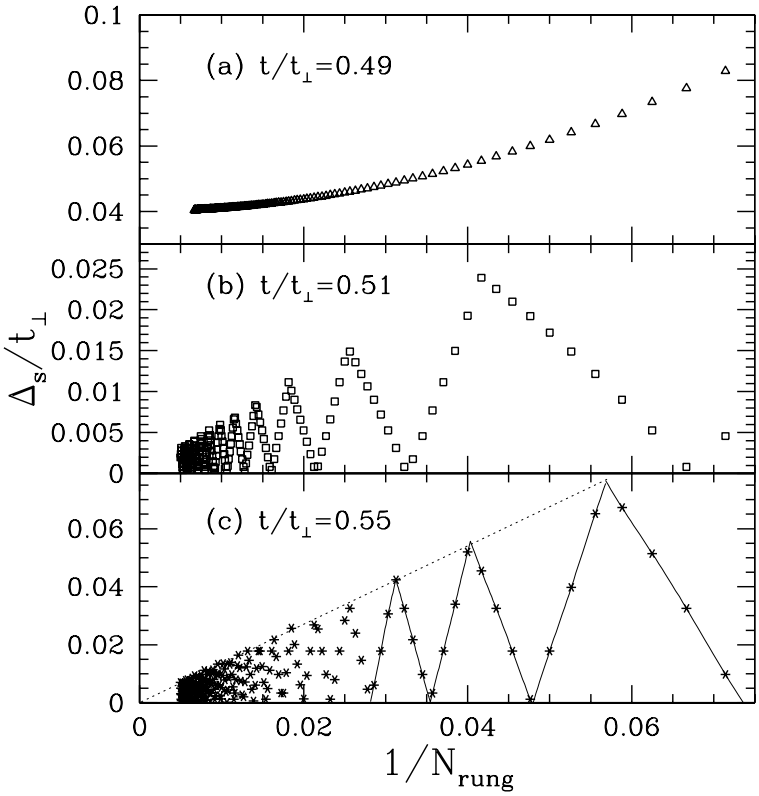

Figure 4. Finite-size scaling of the spin gap Δ_s in the non-interacting case ($U = 0$) for $t/t_\perp = 0.49$ (a), $t/t_\perp = 0.51$ (b) and $t/t_\perp = 0.55$ (c). These are exact results for open lattices.

for a system with a small gap. This is illustrated in figure 5 for the $t/t_\perp = 0.6$ case, where a crossover to linear behaviour is observed as the lattice size reaches around 30 rungs. As mentioned, it is important to first assess the DMRG convergence for the finite lattices before attempting extrapolations. In table 4, we show the DMRG convergence of Δ_s with m for the odd-rung algorithm, with m ranging from 200 to 1500. It can be seen in this case that the finite-lattice estimates are sufficiently well converged to afford reliable extrapolations. In figure 5 results from the odd-rung algorithm with $m = 750$ are plotted along with results from

Table 4. DMRG convergence of the spin gap $\Delta_s/t_\perp$ with m, the number of states retained per block, for the odd-rung algorithm, where the ground and first excited states are included in the density matrix with equal weights. The parameters used are $U/t_\perp = 1, t/t_\perp = 0.6$.

N_{rung}	$m = 200$	$m = 370$	$m = 580$	$m = 750$	$m = 1200$	$m = 1500$
3	0.2371380	0.2371380	0.2371380	0.2371380	0.2371380	0.2371380
7	0.1115510	0.1115030	0.1115060	0.1115040	0.1115010	0.1115010
13	0.0675853	0.0673585	0.0672920	0.0672718	0.0672626	0.0672597
19	0.0475570	0.0475439	0.0475508	0.0475459	0.0475420	0.0475383
25	0.0382940	0.0383589	0.0383977	0.0384008	0.0384094	0.0384077
31	0.0333642	0.0335102	0.0336259	0.0336437	0.0336687	—
35	0.0314530	0.0317155	0.0319372	0.0319716	0.0320189	—

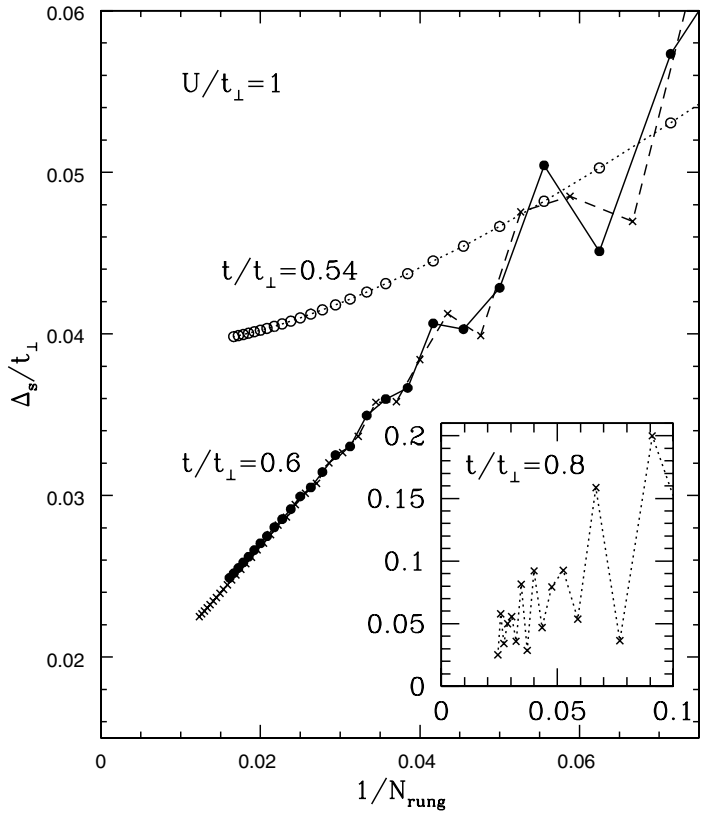

Figure 5. Finite-size scaling of the spin gap Δ_s for $U/t_\perp = 1$ and $t/t_\perp = 0.54$, 0.6, obtained from DMRG calculations. For $t/t_\perp = 0.6$, the results from the two different DMRG algorithms: odd rungs (crosses) and even rungs (full dots), retaining 750 and 800 states per block respectively, are compared. The inset shows the FSS in the $U/t_\perp = 1$, $t/t_\perp = 0.8$ case using the odd-rung DMRG algorithm with $m = 1200$.

the even-rung algorithm with $m = 800$. Good agreement can be seen between the two sets of results in the linear regime. In order to make bulk estimates for $t/t_\perp \geqslant 0.6$, we assume a linear scaling *ansatz*. Presumably, if the resulting estimate is non-zero, as is the case, e.g., for $t/t_\perp = 0.6$, there should be a crossover from linear to quadratic scaling for larger lattices still, in which case the estimates are (tight) lower bounds on the spin gap. For the case of $U/t_\perp = 1$, we can carry this out until $t/t_\perp$ reaches around 0.75. Beyond this value, the FSS is too erratic to permit accurate finite-lattice estimates of the spin gap for sufficiently large lattices. In the inset to figure 5 this erratic FSS is shown for the $t/t_\perp = 0.8$ case.

Plots of the DMRG bulk estimates of Δ_s as functions of $t/t_\perp$ are included in figure 3. The spin gap obtained in this way is indistinguishable from the series values for small t. However, the DMRG calculation also provides well converged results for larger t provided that U is not too small. In the $U/t_\perp = 2$ case, for example, Δ_s undergoes a very rapid decrease up to $t/t_\perp \simeq 0.6$, and then flattens out at a small but finite value. The same behaviour was already seen in the previous DMRG calculation of Noack *et al* [11]. Noack *et al* [11] did their calculation at a fixed lattice size 2×32 sites, however, whereas we performed a careful finite-size scaling analysis to confirm that the spin gap remains finite, rather than scaling to zero in the bulk limit.

In the $U/t_\perp = 1$ case, a similar effect occurs, but the FSS behaviour becomes completely erratic and the extrapolations fail at around $t/t_\perp \approx 0.75$. In figure 6 we depict the region in the $(U/t_\perp)$–$(t/t_\perp)$ plane where the DMRG calculation either fails to give reasonable results due to erratic FSS, or indicates a very small or vanishing gap, by marking it with an 'F'. Also included in figure 6 is the line where the series appear to give a vanishing spin gap. This line indicates the crossover in the physics of the system from band insulator to strongly correlated Mott insulator.

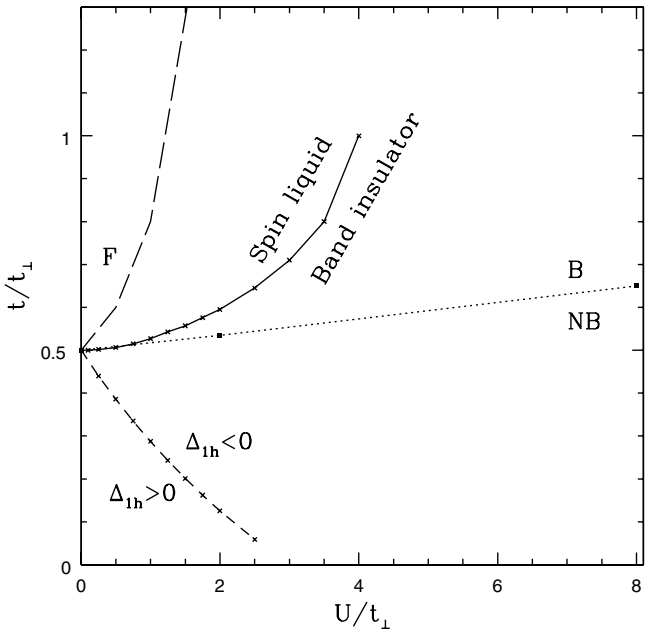

Figure 6. Phases and critical lines for the Hubbard ladder at half-filling, in the plane of $U/t_\perp$ versus $t/t_\perp$ (see the text). The phase boundary between spin liquid and band insulator is obtained approximately by determining the position where the spin gap vanishes according to the series. The region where two holes bind (do not bind) is marked by B (NB). The region in which the DMRG calculation fails to determine whether the system has a spin gap, due the irregular finite-size scaling, is marked by F. Also marked is the region where the one-hole gap is positive/negative.

4. One- and two-hole states

As mentioned in section 1 there is considerable interest in the doped Hubbard ladder where the electron density $n < 1$. The series method is not well suited to studying the effect of finite doping. However, we are able to compute the ground-state and excitation energies when the system contains one or two holes.

4.1. The one-hole case

In the $t = 0$ limit a single hole will change one of the singlet rung states into an $S^z = \frac{1}{2}$ or $-\frac{1}{2}$ bonding state, with an energy increase of $-t_\perp - \lambda_1$. Finite t will allow the hole to propagate along the ladder, giving a quasiparticle band. Figure 7 shows the quasiparticle excitation energy $\Delta_{1h}/t_\perp$ as a function of wavenumber for the case $t/t_\perp = 0.5$ and various $U/t_\perp$. For

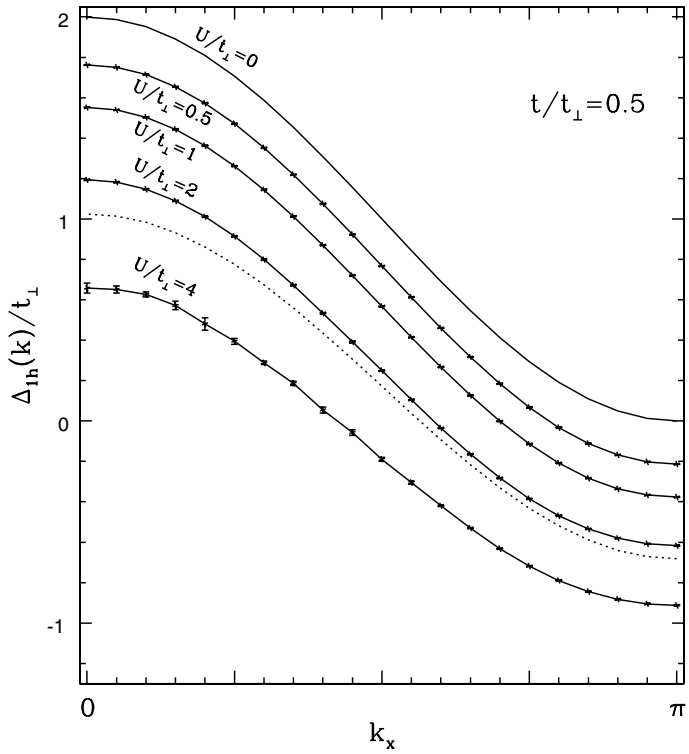

Figure 7. Excitation spectra for one-hole bonding states for $t/t_\perp = 0.5$ and various $U/t_\perp$, obtained from series expansions. Also shown are the results from the local rung approximation [14] at $U/t_\perp = 4$ (dashed line).

$U = 0$ we have the exact results

$$\Delta_{1h}(k) = t_\perp + 2t\cos(k) \tag{8}$$

and this is seen through the vanishing of all higher terms in the series. For the choice $t/t_\perp = 0.5$ this gives $\Delta_{1h} = 0$ at $k = \pi$. We also show, for comparison, the approximate dispersion curve for $U/t_\perp = 4$ obtained by Endres *et al* [14], through their 'local rung approximation'. This appears to overestimate the energy by about $0.4t_\perp$, although the overall shape is very similar.

For increasing U the energies are depressed and there is a small decrease in the quasiparticle bandwidth although the overall cosine shape remains. The minimum of the quasiparticle spectrum occurs at $k = \pi$ throughout. The energy zero is taken to be the ground-state energy of the half-filled ladder. Each quasiparticle band crosses the zero level, indicating that the overall energy of the system is reduced when a hole is created, and this is also marked in figure 6. Figure 8 shows the 'quasiparticle gap' as a function of $t/t_\perp$ for various $U/t_\perp$ obtained from the series and DMRG methods. Both methods agree up to $t/t_\perp \sim 0.5$, beyond which the series fail to converge. This is the same crossover region as seen in the spin-gap studies. The DMRG results suggest an upturn or change in slope for larger $t/t_\perp$ and $U/t_\perp$ not too large, as shown in the figure for $U/t_\perp = 1$ or 2. Further evidence is shown in figure 9, where we plot the finite-lattice results versus $1/N^2$. There is a very distinct upturn from $t/t_\perp$ equals 0.52 to 0.54. By $t/t_\perp = 0.6$, however, the irregular sawtooth behaviour has set in once again, and no very reliable finite-size scaling extrapolation could be made. Noack *et al* [11] saw a similar break in the behaviour of the charge gap at the crossover for $U/t_\perp = 4$.

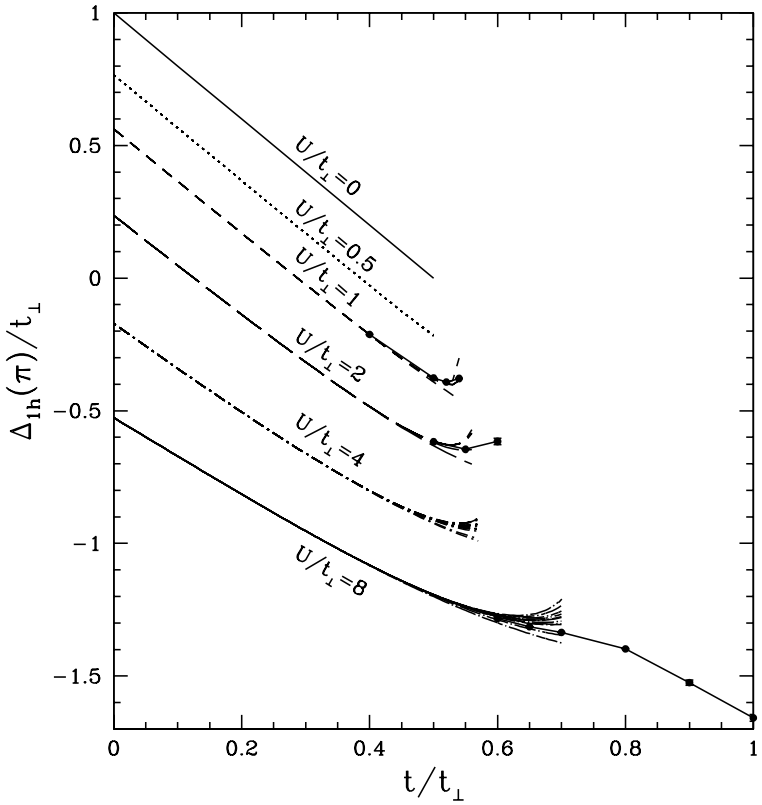

Figure 8. The one-hole 'quasiparticle gap' as a function of $t/t_\perp$ for various $U/t_\perp$. The dashed lines are the extrapolations of the series using the different integrated differential approximants, while the points connected by solid lines are the results of DMRG calculations. Also shown are the exact results for the case $U = 0$.

4.2. The two-hole case

We would also like to explore the system doped with two holes, to see whether binding occurs between the holes. From table 1, one can see that at zeroth order ($t = 0$), the energy gap for two holes sitting on the same rung is $\frac{1}{2}[\sqrt{(U^2 + 16t_\perp^2)} - U]$, which is larger than the gap $[\sqrt{(U^2 + 16t_\perp^2)} - U] - 2t_\perp$ for two holes on different rungs. Thus it is not energetically favourable to have two holes on the same rung. Our present series methods, unfortunately, are unable to treat the latter case of two holes on separate rungs: so here we restrict ourselves to exploring whether the former state becomes bound at larger t. One starts from a state with both holes on a single rung and all other rungs in spin-singlet states; and then the hopping term allows these holes to move along the ladder, and so generates a dispersion relation for this state. For example at $U/t_\perp = 8$, our second-order series result for the dispersion is

$$\Delta_{2h}(k)/t_\perp = 0.4721 + (1.805 + 1.447\cos k)(t/t_\perp)^2. \tag{9}$$

One can see that the minimum energy is at $k = \pi$, rather than 0, due to the fact that this is not the lowest-energy two-hole state. Comparing with the one-hole dispersion relation, we find no evidence for binding of this state at higher t.

Our series results do not preclude the existence of a two-hole bound state of more complex structure, and there are indications from other work that this can occur. Noack *et al* [10, 11]

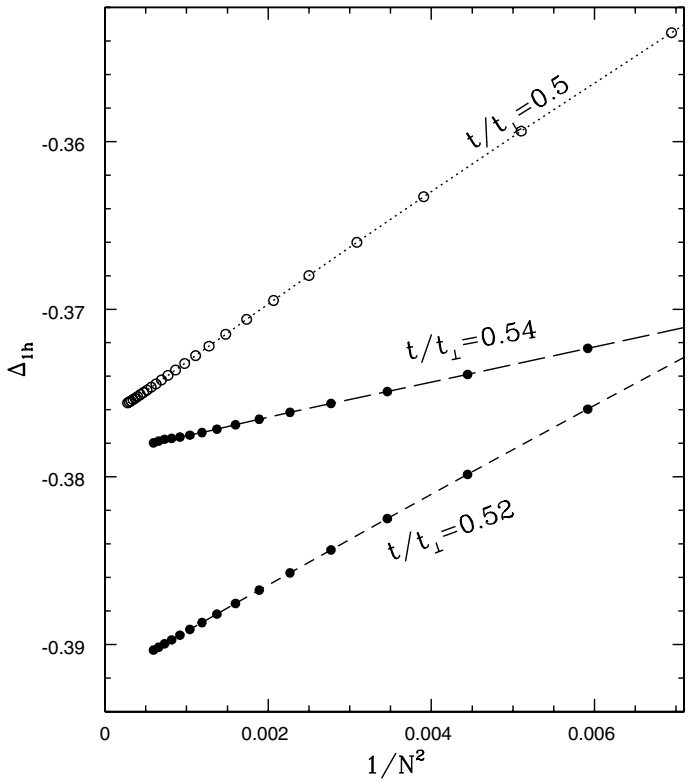

Figure 9. The one-hole 'quasiparticle gap' $\Delta_{1h}(\pi)$ for $U/t_\perp = 1$ and $t/t_\perp = 0.5, 0.52, 0.54, 0.6$, as a function of $1/N^2_{\text{rung}}$, obtained from DMRG calculations.

find, for a 2×32 lattice, a small binding energy ($E_b \simeq 0.14$) for two holes, and a pair wavefunction which has roughly equal amplitudes on a rung and between nearest neighbours along the same leg of the ladder. Finite-size effects may be large enough to mask the true behaviour. Kim *et al* [22] also discuss pair formation using both the DMRG and a variational method. They conclude that, at least for large U, holes favour adjacent rungs to minimize the Coulomb energy. Our series method is unable to explore such complex pair states.

Instead, we have used the DMRG method to compute the minimum energy of the system with one and two holes, up to ladders of size $2 \times L$ ($L = 60$), and hence the binding energy defined by

$$E_b = 2[E_0(L, L-1) - E_0(L, L)] - E_0(L-1, L-1) + E_0(L, L) \qquad (10)$$

where $E_0(N_\uparrow, N_\downarrow)$ is the ground-state energy with $N_\uparrow$ ($N_\downarrow$) up (down) electrons. We show this as a function of $t/t_\perp$ for $U/t_\perp = 2, 8$ in figure 10. As can be seen, there is no binding for small $t/t_\perp$, and the binding energy is zero, corresponding to an unbound, well separated pair of holes.

For $t/t_\perp$ larger than a critical value $(t/t_\perp)_c$, however, hole binding does occur. In fact as we can see from figure 10, the binding energy E_b increases from zero very rapidly beyond the critical $(t/t_\perp)_c$. The binding is especially strong at small $U/t_\perp$, and weakens as $U/t_\perp$ increases. The boundary for two-hole binding is shown in our 'phase diagram', figure 6.

Now the binding of two holes is expected to be a necessary though not sufficient pre-condition for the phenomenon of phase separation (binding of many holes). Phase separation

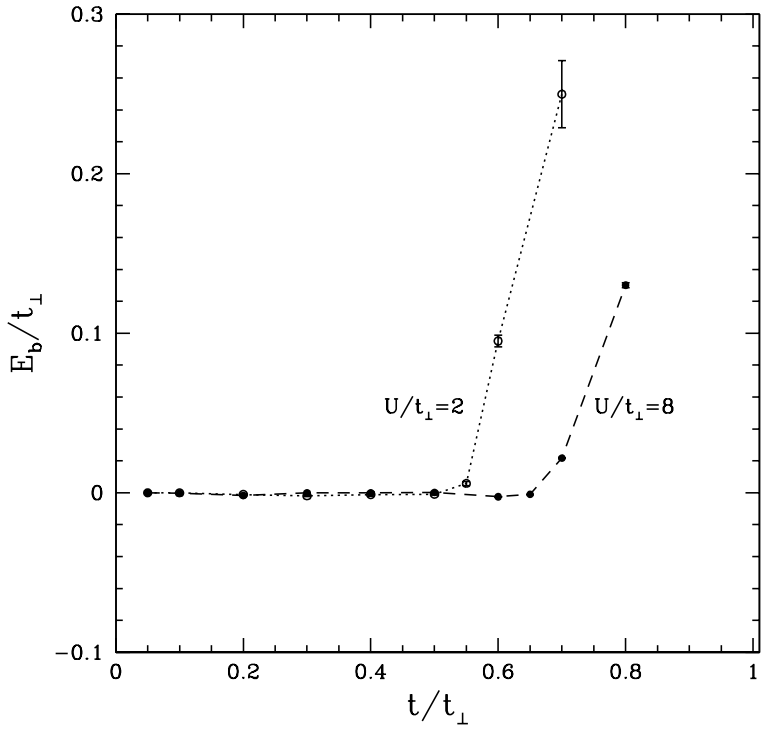

Figure 10. Binding energy E_b of two holes versus $t/t_\perp$ for various $U/t_\perp$, obtained from DMRG calculations.

is known to occur for the t–J ladder [2, 3], but no evidence for it has yet been found in the Hubbard ladder, as far as we are aware. It could be interesting to search for this phenomenon in the region indicated above.

5. Discussion and conclusions

We have made the first application of the series expansion method to the Hubbard model on a two-leg ladder, and also used the DMRG method to explore its properties at half-filling and at $T = 0$. Our series approach starts from a basis of rung states, appropriate for small values of the chain hopping parameter t, and we obtain perturbation series for various quantities in powers of t up to typically ten terms. The series are well behaved out to typically $t/t_\perp \sim 0.6$. but the convergence becomes problematical beyond that point. Our results are complementary to both analytical weak-coupling calculations and other numerical (DMRG and QMC) results. We also present a detailed discussion of the finite-size scaling behaviour of the model using the DMRG, in order to check for any phase transitions.

We have calculated the ground-state energy and the triplet spin-excitation energies at half-filling, and the excitation energies of one-hole and two-hole states relative to the half-filled case. At half-filling the system is believed to be in a spin-gapped insulating phase [8, 11] for all values of the parameters $U, t_\perp$. Our results confirm those of Noack *et al* [11], showing a sharp crossover at smaller $U/t_\perp$ from strongly correlated spin liquid or Mott insulator (as for a simple Hubbard chain) to 'band insulator' behaviour as $t_\perp$ is increased. The spin gap becomes very small in the spin-liquid region. We have performed a careful finite-size scaling analysis using

the DMRG to show that the spin gap remains finite, however, rather than scaling to zero in the bulk limit, at least for those moderate values of $U/t_\perp$ where a definite statement is possible. In other words, no evidence of a second-order phase transition was found for finite $U/t_\perp$.

A single hole doped into the Hubbard ladder will propagate as a well defined quasiparticle, and we have computed the dispersion relation for this quasiparticle. It was found that the lowest-energy two-hole state is not amenable to our series approach; but the DMRG calculations show that two holes become strongly bound at larger $t/t_\perp$. This raises the question of whether phase separation will occur in this region, as it does in the t–J ladder [23]. This question must await future investigations.

Acknowledgments

This work forms part of a research project supported by a grant from the Australian Research Council. One of us (RJB) would like to thank Dr William Barford for co-development of one of the DMRG codes. We would also like to thank Dr Reinhard Noack for sending us his DMRG results for comparison. The computation has been performed on Silicon Graphics Power Challenge and Convex machines. We thank the New South Wales Centre for Parallel Computing for facilities and assistance with the calculations.

References

[1] Azuma M, Hiroi Z, Takano M, Ishida K and Kitaoka Y 1994 *Phys. Rev. Lett.* **73** 3463
Hiroi Z and Takano M 1995 *Nature* **377** 41
The material $(VO)_2P_2O_7$ which was originally described as a spin ladder has been shown to be better described as a fully two-dimensional structure; see e.g.
Uhrig G S and Normand B 1998 *Phys. Rev.* B **58** R14 705
[2] Dagotto E and Rice T M 1996 *Science* **271** 618
[3] Uehara M *et al* 1996 *J. Phys. Soc. Japan* **65** 2764
[4] Müller T F A and Rice T M 1998 *Phys. Rev.* B **58** 3425
[5] Fabrizio M, Parola A and Tosatti E 1992 *Phys. Rev.* B **46** 3159
See also
Varma and Zawadowski 1985 *Phys. Rev.* B **32** 7399
[6] Bourbonnais C and Caron L G 1991 *Int. J. Mod. Phys.* B **5** 1033 and references therein
[7] Khveshchenko D V and Rice T M 1994 *Phys. Rev.* B **50** 252
[8] Balents L and Fisher M P A 1996 *Phys. Rev.* B **53** 12 133
[9] White S R 1992 *Phys. Rev. Lett.* **69** 2863
White S R 1993 *Phys. Rev.* B **48** 10 345
[10] Noack R M, White S R and Scalapino D J 1994 *Phys. Rev. Lett.* **73** 882
Noack R M, Bulut N, Scalapino D J and Zacher M G 1997 *Phys. Rev.* B **56** 7162
[11] Noack R M, White S R and Scalapino D J 1996 *Physica* C **270** 281
[12] Park Y, Liang S and Lee T K 1999 *Phys. Rev.* B **59** 2587
[13] Riera J, Poilblanc D and Dagotto E 1999 *Eur. Phys. J.* **137** 53
[14] Endres H, Noack R M, Hanke W, Poilblanc D and Scalapino D J 1996 *Phys. Rev.* B **53** 5530
[15] Gelfand M P, Singh R R P and Huse D A 1990 *J. Stat. Phys.* **59** 1093
[16] He H X, Hamer C J and Oitmaa J 1990 *J. Phys. A: Math. Gen.* **23** 1775
[17] Gelfand M P 1996 *Solid State Commun.* **98** 11
[18] Hamer C J, Zheng W H and Oitmaa J 1998 *Phys. Rev.* B **50** 15 508
[19] Oitmaa J, Hamer C J and Zheng W H 1999 *Phys. Rev.* B **60** 16 364
[20] Shi Z P and Singh R R P 1995 *Phys. Rev.* B **52** 9620
Shi Z P and Singh R R P 1995 *Europhys. Lett.* **3** 219
[21] Guttmann A J 1989 *Phase Transitions and Critical Phenomena* vol 13, ed C Domb and M S Green (New York: Academic)
[22] Kim E H, Sierra G and Duffy D 1999 *Phys. Rev.* B **60** 5169
[23] Rommer S, White S R and Scalapino D J 2000 *Phys. Rev.* B **61** 13 424